

# Spatiotemporal Structure of Magnetic Field and Convection Vortices Generated in a Rotating Spherical Shell

ISHIHARA Norio and KIDA Shigeo<sup>1</sup>

Faculty of Science, Nagoya University, Nagoya 464-8602, Japan

<sup>1</sup> National Institute for Fusion Science, Toki 509-5292, Japan

(Received: 11 December 2001 / Accepted: 20 June 2002)

## Abstract

Intensification mechanisms of magnetic field by thermal convection in a rotating spherical shell are investigated by the direct numerical simulation analysis of the MHD Boussinesq equation. It is found that an axial magnetic dipole field whose energy is 15 times as large as the kinetic energy is generated. Anticyclonic vortices play a key role in sustaining the structure.

## Keywords:

dynamo, MHD, vortex, spherical shell, thermal convection

## 1. Introduction

In recent years, much progress has been made in our understanding of the origin of the geomagnetic field which is believed to be generated by thermal convective motion of an electrically conducting fluid in the outer core. Many research groups have discussed the mechanisms from the point of view of the formation of loops in magnetic lines of the mean structure averaged over the longitudinal direction (see ref. [1] for a recent review). Unfortunately, however, this mean-field approach misses an instantaneous localized structure and time-dependence of dynamo magnetic field. It is not well understood how the spatial structure of magnetic field develops if it starts with a weak seed of magnetic field because of complexity of the dynamo magnetic field. It is indispensable to clarify these dynamical behavior in understanding the fundamental mechanism. In order to capture the behavior, spatiotemporal structure of magnetic field is investigated, with particular attention to the region of maximal field strength.

## 2. Formulation

We consider a dynamo action driven by thermal convection in a rotating spherical shell. It is assumed that an electrically conducting fluid is confined between two concentric spheres of radii  $r_i$  and  $r_o$  which are rotating at a common constant angular velocity. Temperature on the inner and outer spheres is uniform in space and constant in time, and the former is higher than the latter. There are vacuum outside the outer sphere and a perfect insulator inside the inner sphere. All the physical quantities of the fluid, such as the density (except in the buoyancy term), the thermal diffusivity, the volume expansion coefficient, the kinematic viscosity, the magnetic diffusivity and the magnetic permeability are assumed to be constant and uniform. The gravity force acts on the fluid in the direction to the center of the sphere. Under the MHD and Boussinesq approximation, dynamics of this system is described by the Navier-Stokes equation, the induction equation and the thermal conduction equation. The boundary condition is imposed on the inner and outer spheres as such that the velocity vanishes, the

Corresponding author's e-mail: ishihara@toki.theory.nifs.ac.jp

©2002 by The Japan Society of Plasma Science and Nuclear Fusion Research

temperature is uniform and constant, and the magnetic field is connected continuously with the outside potential fields. We solve the governing equations using spectral method based on the Chebyshev polynomial/spherical harmonic expansion as an initial value problem. Time integration is performed by the use of the Crank-Nicolson/Adams-Basforth scheme. The Chebyshev tau method is employed in order to satisfy the boundary conditions (see ref. [2] for more details of the numerical scheme).

### 3. Results

The present system is characterized by five nondimensional parameters, that is, the ratio  $r_i/r_o$  of the radii of the inner and outer spheres, the Taylor number  $Ta$ , the Rayleigh number  $Ra$ , the Prandtl number  $Pr$ , the Strebor number  $St$ . A direct numerical simulation is performed in two steps<sup>1</sup>. In the first step, the problem of thermal convection without magnetic field is solved, adding a uniform random small perturbation to a slightly unstable thermal conduction state with parameters  $r_i/r_o = 0.5$ ,  $Ta = 1.6 \times 10^6$ ,  $Ra = 3.2 \times 10^4$ ,  $Pr = 1$ . Nine pairs of cyclonic and anticyclonic vortices appear alternately around the rotation axis. A cyclonic (an anticyclonic) vortex has the same (opposite) direction as (to) the rotation of this shell.

In the second step, dynamo simulations are performed, by adding small magnetic perturbations to the thermal convection field for various values of  $St$ . There is a critical Strebor number below which dynamo action is effective. This critical Strebor number is 0.149 for the present set of parameters. In the following, we report the results of  $St = 0.1$ . Figure 1 shows temporal evolution of total kinetic energy and total magnetic energy integrated over the entire space. There are three distinct periods classified by the temporal variation of the magnetic energy, that is, the linear growing ( $1 < t < 26$ ), the first equilibrium ( $28 < t < 38$ ) and the second equilibrium ( $t > 43$ ) periods. The mechanism and the place of magnetic field intensification are different in the respective periods.

The typical structure of strong magnetic field is shown in Fig. 2. Gray and white surfaces represent isosurface of magnitude of magnetic field and vorticity, respectively. The axial component of vorticity on the equatorial plane is drawn by black lines for cyclone ( $\omega_z$

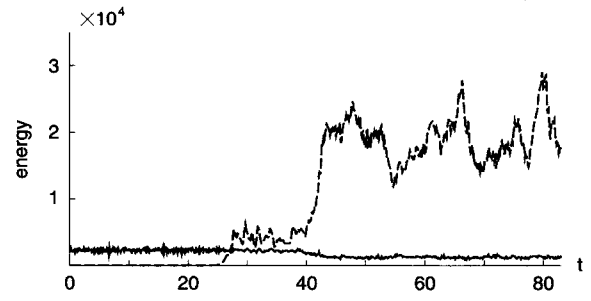
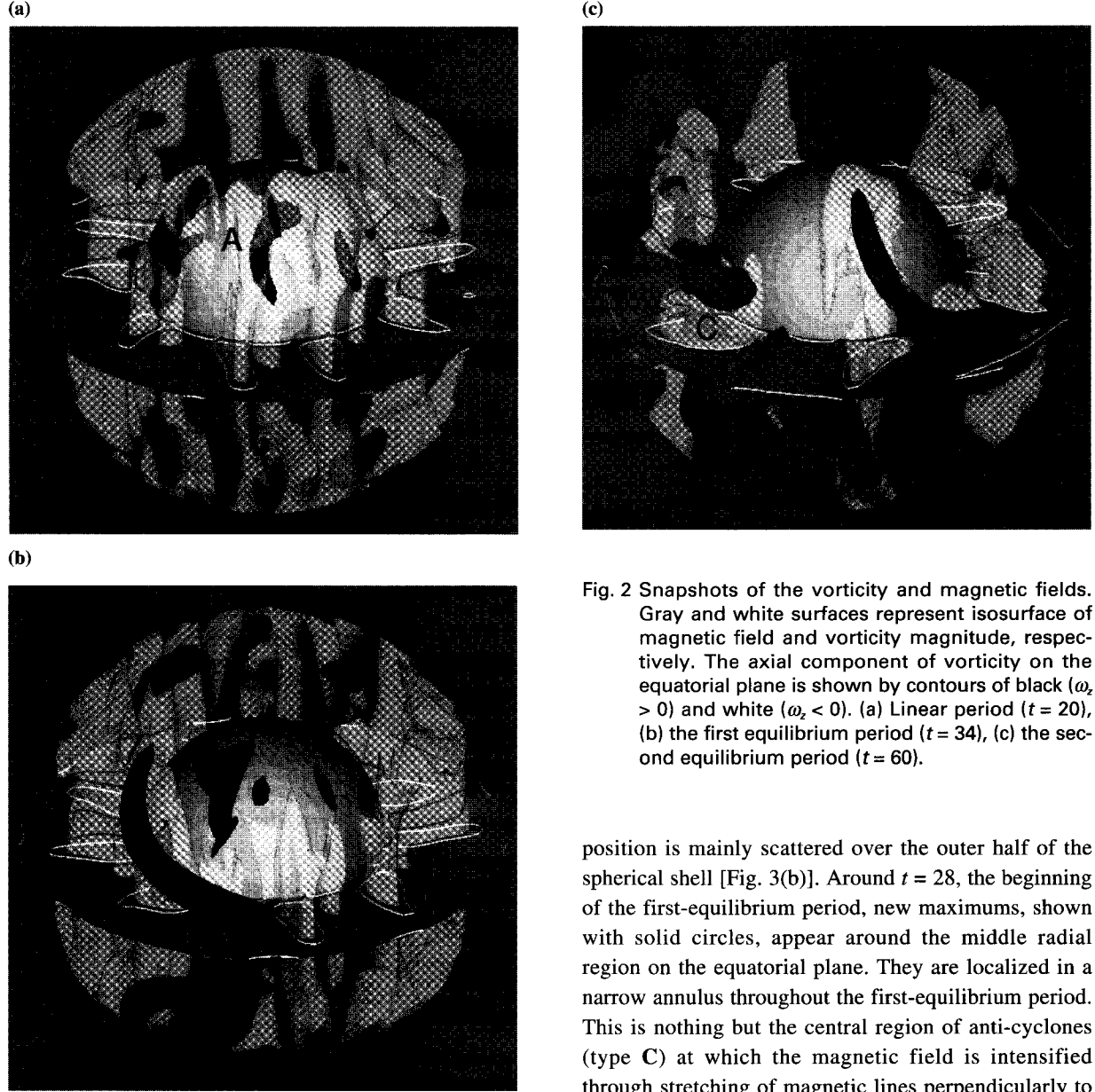


Fig. 1 Temporal evolution of total kinetic energy (solid line) and total magnetic energy (dashed line) integrated over the entire space.

$> 0$ ) and white lines for anticyclone ( $\omega_z < 0$ ). In the linear period, cigar-shaped regions of strong magnetic field are observed between cyclones and their western neighboring anti-cyclones off the equatorial plane at middle latitude [type A, Fig. 2(a)]. In the first equilibrium period, strong magnetic field is generated between anticyclone and outer sphere, inside of anticyclones in addition to the place observed in the linear period [Fig. 2(b)]. Banana-shaped blobs are located between anticyclones and outer sphere (type B). Cigar-shaped ones parallel to the rotation axis are located inside anticyclones (type C). Interestingly, these blobs always appear together, as reported in [3]. In the second equilibrium period, the magnetic field is strong inside anticyclones (type C), as well as between these vortices and the outer sphere (Type B) and eastside of anticyclones (type D). See ref. [3] for magnetic field structure outside the outer sphere.

In order to capture the dynamics, we take an overview of the most intensified locations of the magnetic field. In Fig. 3, we plot (a) the latitudinal and (b) the radial positions of the maximum of  $|b_z|$  over the whole simulation period, respectively. The maximums are searched in each hemisphere separately since the field is nearly symmetric with respect to the equatorial plane. Different symbols distinguish the areas of locations of the maximums. They are divided into three in the temporal and latitudinal plane, namely, the regions of higher latitude than  $20^\circ$  both in the northern and southern hemispheres at earlier times  $t < 40$  and the rest. The former two are distinguished with crosses  $\times$

<sup>1</sup> There are a couple of ways to carry out an MHD dynamo simulation. For example, it is simulated by adding perturbations in both temperature and magnetic fields to an unstable thermal conduction state. Another one is to start with a perturbed unstable thermal conduction state under a given magnetic field and to remove the imposed magnetic field after some temporal evolution.



**Fig. 2** Snapshots of the vorticity and magnetic fields. Gray and white surfaces represent isosurfaces of magnetic field and vorticity magnitude, respectively. The axial component of vorticity on the equatorial plane is shown by contours of black ( $\omega_z > 0$ ) and white ( $\omega_z < 0$ ). (a) Linear period ( $t = 20$ ), (b) the first equilibrium period ( $t = 34$ ), (c) the second equilibrium period ( $t = 60$ ).

and open circles  $\circ$ , respectively. The rest is divided further into two by the radial coordinate, i.e. the middle region (solid circle  $\bullet$ ) and the outer-sphere side (square  $\square$ ).

It is seen in Fig. 3 that the maximum are localized at the middle latitude ( $37^\circ \pm 6^\circ$ , where  $\pm$  denotes the standard deviation) from the beginning through the end of the first-equilibrium period. The maximum distributes symmetrically, in the statistical sense, in the northern and southern hemispheres. These are the strong magnetic field intensified between cyclones and their western neighboring anti-cyclones (type A). Their radial

position is mainly scattered over the outer half of the spherical shell [Fig. 3(b)]. Around  $t = 28$ , the beginning of the first-equilibrium period, new maximum, shown with solid circles, appear around the middle radial region on the equatorial plane. They are localized in a narrow annulus throughout the first-equilibrium period. This is nothing but the central region of anti-cyclones (type C) at which the magnetic field is intensified through stretching of magnetic lines perpendicularly to the equatorial plane. Coexistence of B and C are the characteristics of the first-equilibrium period. Later, in the second-equilibrium period ( $t > 43$ ) these maximum positions C spread out more in both the latitudinal and radial directions, which is the manifestation of more violent activity of the magnetic field. As reported in ref. [3], a recurrent interaction between convection vortices and magnetic field is observed in this period. While the crosses and open circles disappear in this period, another group of maximum (shown by squares) appear near the outer boundary and at low latitude ( $30^\circ \pm 3^\circ$ ), which corresponds to the banana-shaped blobs of strong magnetic field intensified along accelerating streamlines

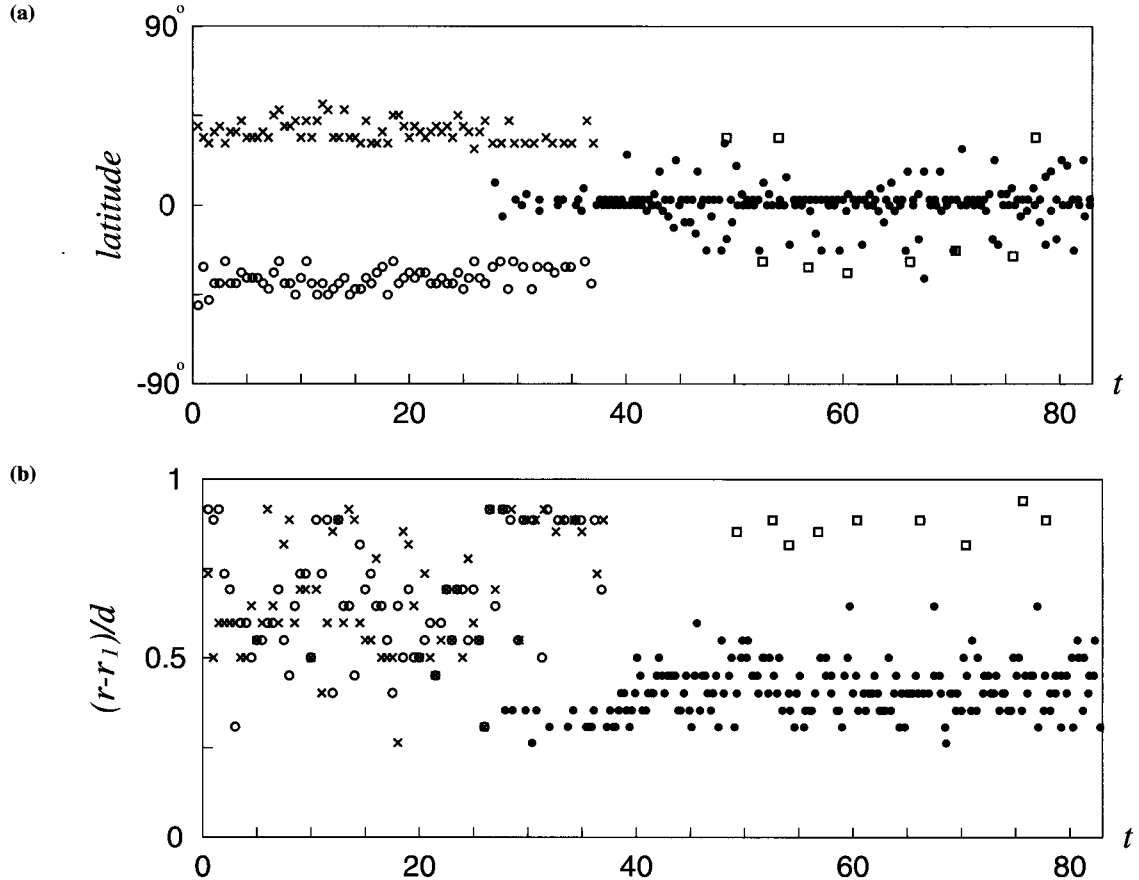


**Fig. 3** The locations of the maximums of  $|b_z|$  are plotted with symbols on (a) the latitudinal and (b) radial coordinates versus time plane. The maximums are searched in each hemisphere separately. Symbols distinguish the areas of locations of the maximums: Cross  $\times$  and open circle  $\circ$  refer to higher latitude than  $20^\circ$  in the northern and southern hemispheres, respectively, at early times ( $t < 40$ ), whereas square  $\square$  and solid circle  $\bullet$  refer to the outer-sphere side and the middle radial regions, respectively.

through the stagnation point just outside of the Ekman boundary layer along the outer sphere (type **B**). Incidentally, type **D** is not observed here because the magnitude of magnetic field is not so large. It is interesting to note that these open squares appear more in the periods of lower magnetic energy ( $50 < t < 60$  and  $70 < t < 80$ ), while they are rare when the activity of the magnetic field is higher ( $40 < t < 50$  and  $60 < t < 70$ ).

#### 4. Summary

In this paper, we have investigated intensification mechanism of magnetic field by thermal convection in a rotating spherical shell with particular attention to the region of maximal field strength. An axial magnetic dipole field whose energy is 15 times as large as the kinetic energy is generated. The magnetic field is intensified in four particular places over all the

simulation period, that is, between cyclones and their western neighboring anticyclones at middle latitude as well as low latitude in the linear period, inside anticyclones, and between anticyclones and the outer boundary in the first and second equilibrium periods.

#### References

- [1] P.H. Roberts and G.A. Glatzmaier, Rev. Mod. Phys. **72**, 1081 (2000).
- [2] H. Kitauchi and S. Kida, Phys. Fluids **10**, 457 (1998).
- [3] N. Ishihara and S. Kida, J. Phys. Soc. Jpn. **69**, 1582 (2000).
- [4] S. Kida and N. Ishihara, J. Plasma Fusion Res. **77**, 355 (2001).
- [5] N. Ishihara and S. Kida, Research Report NIFS, NIFS-708 (2001).